

A comparison of dioxygen bond-cleavage in ribonucleotide reductase (RNR) and methane monooxygenase (MMO)

Per E.M. Siegbahn *

*Department of Physics, Stockholm Centre for Physics, Astronomy and Biotechnology (SCFAB), Stockholm University,
S-106 91 Stockholm, Sweden*

Received 29 June 2001; in final form 7 November 2001

Abstract

The O₂ cleavage by the iron dimer complex in RNR is experimentally found to be at least 400 times faster than the one in MMO, in spite of very similar iron dimers. The origin of this difference is investigated using the hybrid density functional method B3LYP with models containing about 60 atoms. The calculations support a suggestion that this difference could be due to the presence of a second sphere tryptophan (Trp48) in RNR. © 2002 Elsevier Science B.V. All rights reserved.

1. Introduction

Ribonucleotide reductase (RNR) and methane monooxygenase (MMO) catalyze two quite different reactions. While RNR effects the conversion of ribonucleotides (RNA building blocks) to deoxyribonucleotides (DNA building blocks), MMO inserts one oxygen of dioxygen into a C–H bond of methane to form methanol. In spite of this difference both enzymes use extremely similar diiron complexes as cofactors. The iron dimer in the R2 protein of RNR, with the X-ray structure [1] shown in Fig. 1, has one aspartate, three glutamate and two histidine ligands. There are also a number of oxygen derived ligands, μ -oxo, hydroxide or water, depending on oxidation states of the iron

atoms. The main difference for MMO is that instead of the aspartate there is another glutamate. There may also be a difference in the number of water ligands. Since both aspartate and glutamate have carboxylate side-chains these two iron dimer complexes should therefore be chemically very similar. In the first phase of the mechanism of both RNR and MMO, a dioxygen molecule is bound and cleaved by the iron complex. Interestingly, the rate of O–O bond cleavage is notably different in these enzymes in spite of the large chemical similarity of the iron complexes. The rate of cleavage for MMO is about 1 s⁻¹ [2], corresponding to a barrier (from transition state theory) of 17 kcal/mol, while for RNR it is at least 400 s⁻¹ [3], corresponding to a barrier of 14 kcal/mol. The subject addressed in the present Letter is the origin of this difference.

The present computational study of MMO and RNR follows a similar strategy as similar previous

* Fax: +46-08-55-37-86-01.

E-mail address: ps@physto.se (P.E.M. Siegbahn).

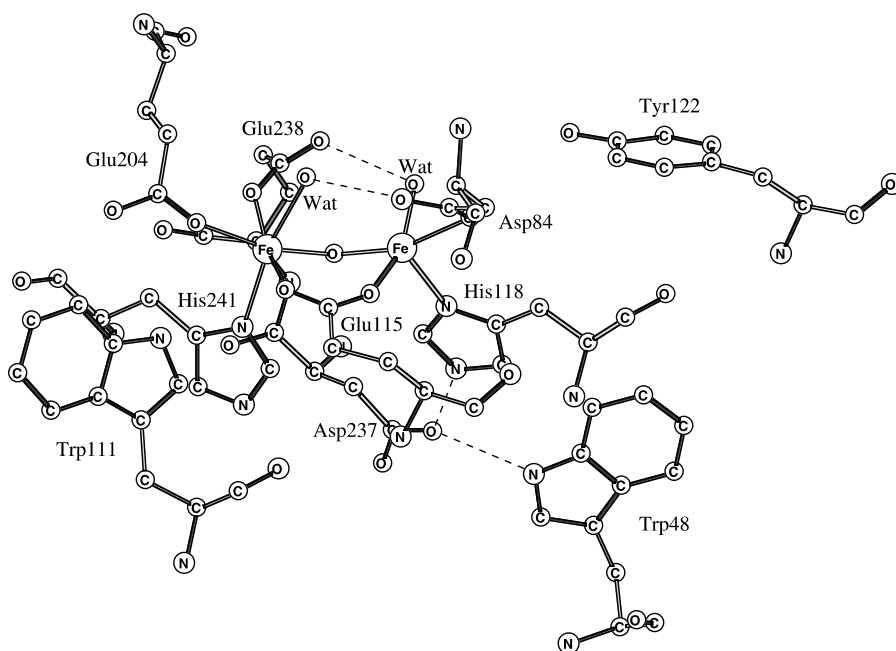


Fig. 1. The region around the Fe(III,III) dimer from the X-ray structure of the R2 protein of RNR [1].

studies [4,5]. The B3LYP method [6] is used with medium size basis sets for the geometries and larger basis sets for the final energies. The initial chemical model used for the iron dimer complexes contains just the first shell ligands. The amino acid ligands are described by their functional groups, imidazoles for the histidines and formates for the carboxylates. As will be shown below, an extension of these models became necessary, where some second sphere amino acids are also included and where the geometry optimization had to be performed using a homogeneous dielectric medium for the surrounding protein.

2. Computational details

The calculations were performed in three steps. For each structure considered, a full geometry optimization was performed using the hybrid density functional B3LYP method [6]. In this first step, standard double zeta basis sets were used for all light elements. For iron a non-relativistic effective core potential (ECP) according to Hay and Wadt [7] was used. The valence basis set used in

connection with this ECP, which is labeled *lacvp* in the JAGUAR program [8], is essentially of double zeta quality. The same basis set was used also for the calculation of the Hessians, for the smaller models where this step was not too time-consuming. In order to keep the structures reasonably close to the X-ray structures some peripheral atoms were locked in their positions as obtained from the experimental structures. The atoms frozen in this way were mostly hydrogen atoms replacing carbon atoms in the real structure. This was done by placing these hydrogen atoms along the C–C bond of the X-ray structure at a distance of 1.10 Å away from the carbon atoms included in the model. A few calculations were made in order to test the adequacy of this procedure by releasing some of the constraints.

In the second step, the B3LYP energy was evaluated at the optimized geometries using a larger basis set, the *lacv3p*** basis set, which is of triple zeta quality and uses a single set of polarization functions on each atom.

In the third step, the surrounding protein was treated with a self-consistent reaction field method, using a Poisson–Boltzmann solver. The dielectric

constant of the homogeneous dielectric medium was set equal to four in line with previous modeling of enzymes [9]. The probe radius was set to 1.40 Å corresponding to the water molecule. Normally, the dielectric effects can be added at the end to the final energies computed as described above. For some of the most important models of the present study that procedure did not work, since convergence to the wrong electronic state was obtained if the reaction field was not included. Therefore, in these cases the geometry had to be performed including the reaction field. The large basis set effects were still taken from the calculations without a dielectric surrounding. Further details are given below. All the calculations were carried out using the JAGUAR program [8].

3. Results and discussion

The present study of O–O bond cleavage in MMO and RNR starts out from a previous study of MMO [10], and the first part of the investigation was to repeat the previous calculations using a slightly different model, see Fig. 2. The only structural difference between the models is that there is a different hydrogen-bonding between a glutamate on one iron center and a water on the other center. Instead of hydrogen bonding with the oxygen closest to iron, the glutamate hydrogen-binds with the outermost oxygen. Another difference is that in the present study also the antiferromagnetic cou-

pling of the irons was investigated, since this is easily achieved using the JAGUAR program.

In the first set of calculations done using the model in Fig. 2, six positions were frozen from their positions in the X-ray structure, one hydrogen for each amino acid ligand according to the procedure described in Section 2. The irons were antiferromagnetically coupled. This resulted in a barrier of 15.0 kcal/mol, which is markedly lower than the 20.4 kcal/mol found in the previous study. The origin of this difference was investigated by first releasing all the constraints from the X-ray structure. This led to a gain of total energy of about 12 kcal/mol, but did not change the barrier significantly, only by 0.4 kcal/mol from 15.0 to 15.4 kcal/mol. There were no significant changes of the geometries either. In the next step of the investigation, ferromagnetic coupling was used. This led to a loss of total energy of about 4 kcal/mol, but the effect on the barrier was again only marginal, from 15.0 to 15.1 kcal/mol. It is therefore concluded that the main reason for the lowering of the barrier in the present study is the different hydrogen bonding used, even though the use of a slightly different basis set could also contribute.

After this preliminary investigation, the rest of the study is focused on the origin of the difference in barrier heights between MMO and RNR. As mentioned in Section 1, the main difference in the first shell ligands between the iron dimer in MMO and RNR is that there is a glutamate in MMO where there is an aspartate in RNR. From the experience gathered so far from modeling metallo-enzymes [5], this difference in length of one of the side chains should not lead to an electronic effect that could explain the difference in barrier heights. In particular, a careful investigation on manganese catalase [11,12] showed that changing the modeling of glutamates, from formates to acetates, led to only very small effects on the relative energies, actually within the convergence thresholds used in the investigation. The same result is found here, and the barrier using the acetate modeling of Asp84 differs from the formate one by only 0.1 kcal/mol. One more comment is needed in this context. Seemingly in contrast to the above conclusion, it has been shown experimentally [13], that if the aspartate to glutamate mutation is made in

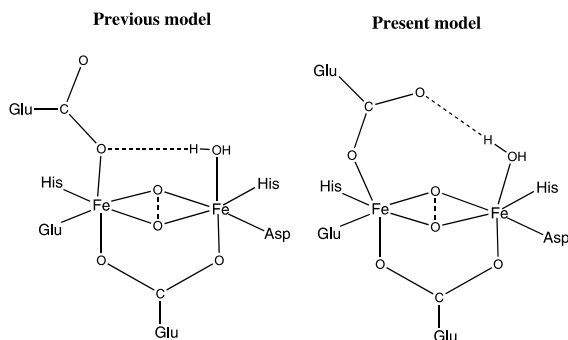


Fig. 2. Previous and present model used to study O–O bond cleavage in RNR and MMO.

RNR, the rate actually goes down to become close to the one in MMO. However, a much more likely explanation for this than an electronic effect, is that the mutated glutamate simply does not fit into the protein framework of RNR. In any mutant, induced protein strain must always be a possible factor influencing the reactivity. The situation is quite different for wild-type enzymes, where evolution in principle can remove the strain. This is supported by calculations [4,5,14], where comparisons between theoretically optimized and experimental wild-type enzyme geometries of active sites have so far shown excellent agreement without any sign of protein strain. This does not necessarily prove that there is no strain in MMO due to the presence of the glutamate and a separate study of this possibility would be of interest. Experimentally, it would also be of interest to investigate the corresponding glutamate to aspartate mutation in MMO, which has not yet been done. A large *positive* effect on the O–O bond cleavage rate from this mutation would clearly demonstrate that protein strain is indeed the origin of the difference between RNR and MMO. From this point on, the interest in the present study was instead centered on the second sphere amino acids, where the electronic differences are larger.

In order to find a possible candidate among the second sphere amino acids for the lowering of the O–O bond cleavage barrier in RNR, the experimentally known details of the reaction between O₂ and the iron dimer have to be recapitulated. The first species observed after this reaction is a compound denoted **X** [15], which has been spectroscopically characterized as an Fe₂(III,IV) complex [16]. Since the reactant with a bound O₂ is an Fe₂(III,III) complex, this means that an outside electron has been transferred to the iron dimer, either directly before, during, or directly after the O₂ activation. In contrast, for MMO the first species observed is compound **Q**, which has been assigned as an Fe₂(IV,IV) complex [17,18]. There are essentially two candidates for the source of the electron in RNR, either Tyr122 or Trp48, see Fig. 1. Until recently, the only known amino acid radical in this region of RNR was Tyr122, which can actually be stable for hours [19]. However, the Tyr122 radical is only observed together with an

Fe₂(III,III) state of the dimer so there must be another electron donor. Recently, Bollinger et al [3] have very convincingly shown that this electron donor is Trp48, and that this radical appears earlier than the Tyr122 radical under normal circumstances. The main candidate for the electron donor in the O₂ reaction in RNR is thus Trp48. This was not entirely unexpected [20], since Trp48 is a part of an amino acid His–Asp–Trp triad found also in Cytochrome C peroxidase (CCP) and in that case a tryptophan radical is observed in the oxidized state [21]. The main scenario investigated here is therefore that an electron comes in from Trp48 to the iron dimer, either before or during the O–O bond cleavage, and increases the rate of this process for RNR. In MMO the tryptophan is not present and the O–O cleavage could therefore be slower for this reason.

The simplest approach to test the possibility that an outside electron would speed up the O–O bond cleavage process is to add an electron to the previous model in Fig. 2, without further extensions. There is one major problem with this approach and this is that the cost for getting the electron from the outside is not obtained. The calculations on the negatively charged model of Fig. 2, using antiferromagnetic coupling, led to a barrier of only 7.6 kcal/mol and an exothermicity of 26.7 kcal/mol. From these results it is clear that a cost for obtaining the additional electron must be involved. Otherwise, the rate would be too fast and the exothermicity too high to be consistent with experiments. Another point worth noting is that the TS O–O bond distance is 1.79 Å which is shorter than the one for the neutral model of 2.05 Å, as expected since the barrier is lower for the negative model.

To reach further, the electron donor has to be included in the model. This means that the model has to be extended by including also Asp237 and Trp48. For this model two solutions should be compared, one where Trp48 is a non-radical and one where it is a radical. For the latter case, three spins should be coupled to a singlet, the two spins on iron antiferromagnetically, and the one on tryptophan. For these two solutions the O–O bond distance was varied in steps, from reactants to products. The maximum along this path is taken

as an approximate transition state, since the system is too big for a calculation of a Hessian. This procedure has been tested in several cases and found to be appropriate for systems like the present one [22].

For the case of the non-radical Trp48 solution the calculation of the reaction path was straightforward. Initially, eight hydrogen atoms were frozen from the X-ray structure, one for each amino acid residue, just as for the smaller model. These C–H bonds replaced C–C bonds in the X-ray structure. For most calculations performed the number of frozen hydrogens were reduced to five marked with X in Fig. 3. Finally, a few calculations were done to investigate the effect of releasing the histidines, where only three hydrogens were consequently frozen.

A major problem occurred when the reaction path was studied for the radical tryptophan. In spite of many different attempts, starting with different structures and wavefunctions, convergence always led to the solution with a non-radical tryptophan. The reason for this problem with the model was concluded to be chemical and not a

technical one of providing the wrong starting guess. One possibility was that the chemical deficiency of the model used was that it did not properly describe the relatively large charge separation which should be present as the tryptophan has donated an electron to the iron dimer. This charge separation could be significantly stabilized by including also the surrounding protein described as a dielectric continuum. This assumption turned out to be correct and when the geometry optimization was redone in a dielectric continuum, convergence to the proper radical solution could successfully be obtained for the product of the O₂ cleavage. Following this solution backwards for shorter O–O distances finally led to an approximate transition state shown in Fig. 3. For much shorter O–O distances convergence to the radical solution still failed, since for these distances the non-radical solution is much lower in energy even in the dielectric continuum. However, this problem does not matter for the present discussion.

The results from the calculations on the mechanism for O–O bond cleavage can be summarized in the following way. For the non-radical

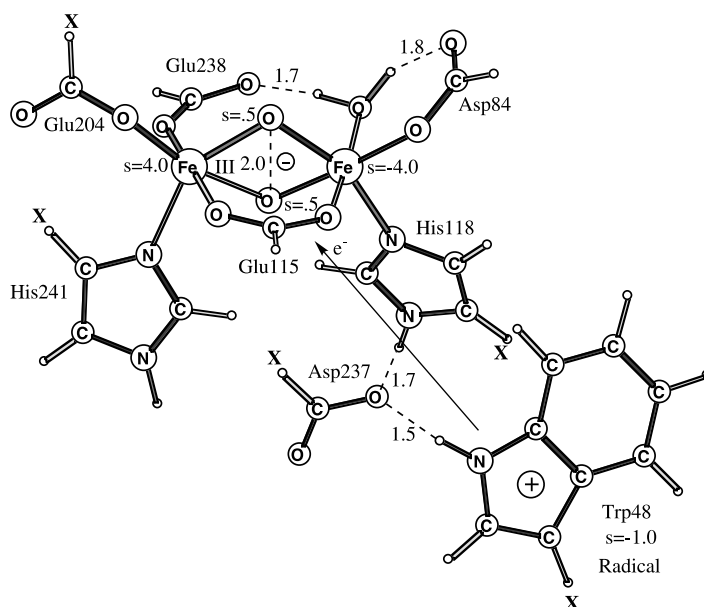


Fig. 3. Approximate transition state structure for O–O bond cleavage in RNR. The optimization is performed with a homogeneous dielectric surrounding with dielectric constant $\epsilon = 4$. Spins larger than 0.1 are given. Atoms marked X are frozen from the corresponding X-ray positions [1].

solution, optimized in a dielectric continuum with five frozen hydrogen coordinates, the barrier is 17.7 kcal/mol. This value was obtained for an O–O distance of 2.05 Å, which is the same as the one fully optimized at the transition state for the smaller model. To be sure that this was actually a transition state, the two oxygen distances to the redox active iron were frozen from the small model. Releasing the histidine positions, reduces the barrier height by 1.4 kcal/mol, to 16.3 kcal/mol. The first product of the reaction is, just as in the previous study [10], an $\text{Fe}_2(\text{III,IV})\text{O}^\cdot$ solution at an energy 9.6 kcal/mol higher than for the reactant (five frozen hydrogens). This solution was not followed further towards the $\text{Fe}_2(\text{IV,IV})$ solution which should eventually be formed at a lower energy. The reactant for this non-radical solution has iron spins of 4.14 and -4.16 , which changes to the transition state values 4.06 and -3.68 .

The product radical solution is found to be better than the non-radical solution by 4.8 kcal/mol, which is thus in line with the experimental observation that an $\text{Fe}_2(\text{III,IV})$ complex (compound **X**) is the first observable product for RNR. The result also supports the conclusion that an electron should be transferred from Trp48 to the iron dimer. This electron transfer should not occur already for the reactant, since at that stage the non-radical solution is lower in energy, but should occur some time later during the O–O bond cleavage.

The radical and non-radical solutions are found to cross for an O–O distance slightly shorter than 2.05 Å, which is the transition state distance for the non-radical solution. A crossing at this distance means that the incoming electron actually lowers the barrier. Even though the accuracy of the present calculations is not high enough to prove that the crossing occurs at this precise distance, they support the suggestion that the electron transfer from Trp48 could be responsible for the lower barrier in RNR compared to MMO.

From the calculated values and the known features of the reactions, an energy diagram for the O_2 cleavage in RNR and MMO can be sketched as in Fig. 4. This diagram was constructed in the

following way. The starting point is the peroxide reactant, denoted **P** in the diagram, where the energy can be set to zero. The energetic positions of **X** and **Q** were set so that the O_2 reactions are a few kcal/mol exothermic. The energies of these states are rather uncertain, but do not matter much for the mechanism. The position of the RNR product is denoted X^- to mark that an electron has been transferred to the iron dimer from Trp48. The corresponding reactant P^- is placed energetically to give the computed reaction energy from the small negative model of -26.7 kcal/mol compared to X^- . The barrier on this surface of 7.6 kcal/mol was also taken from the small negative model. The barrier for the non-radical solution was taken from the result using the large model of 16.3 kcal/mol. The crossing point between the curves was finally taken to occur slightly before the transition state for the non-radical solution, as found in the investigation of the reaction path described above. The MMO

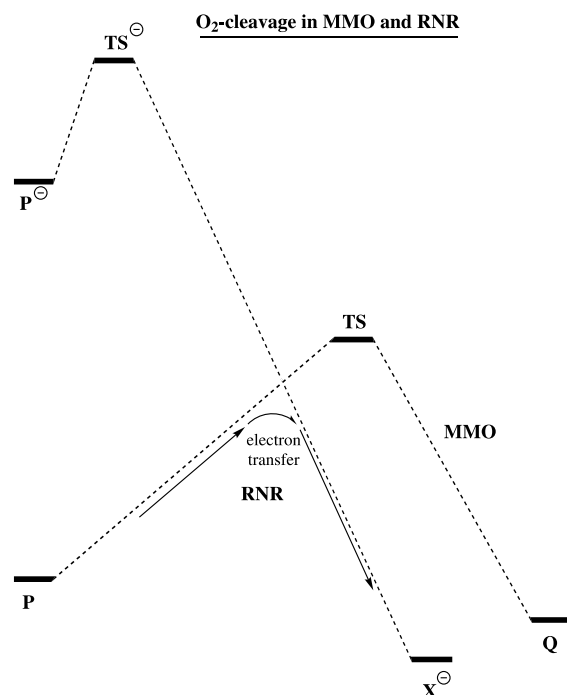


Fig. 4. Energy diagram comparing the O–O bond cleavage in MMO and RNR.

reaction would then simply follow the non-radical solution since no electron enters from the outside. The RNR reaction, on the other hand, starts out along the same non-radical solution as for MMO, but hits the crossing point to the radical solution where the electron transfer occurs from Trp48. From this point the RNR reaction follows the radical solution and it will therefore have a slightly lower barrier than MMO.

Since an electron transfer is implied for RNR it is important that the reorganization energy is low for this mechanism to be efficient. This means that the geometric structures of the radical and non-radical solutions should be very similar. A key here is that the proton stays on tryptophan even after the electron transfer, which is indeed found to be the case in the present geometry optimization including the dielectric continuum. In a test on the separate His–Asp–Trp triad, the proton was found to stay on tryptophan only if the dielectric effects were included in the geometry optimization. The ability of tryptophan to keep its proton also after it is ionized makes it very suitable in electron transfer situations like these. In contrast, a tyrosine will always lose its proton after it is ionized and this therefore makes it less useful for fast electron transfer. The origin of this difference between tyrosine and tryptophan is the presence of the efficient N^+ resonance in tryptophan which actually leads to a radical with the highest spin (about 0.50) on a carbon, the carbon closest to the point marked **X** in Fig. 3.

The prediction that Trp48 is important for the O–O bond cleavage in RNR can finally be compared to experimental findings for the W48F mutant [23]. In line with this prediction, the O–O bond cleavage for the W48F is significantly slower than for the wild-type enzyme, 6–10 s^{-1} compared to more than 400 s^{-1} . However, a rather surprising finding in this experiment is that the peroxy-complex does not build up as it does for the D84E mutant [13]. One possibility could be that the W48F and D84E mutants also affect the rate of formation of the peroxy-complex. Other interpretations of this experiment are obviously also possible, even those advocating no importance for Trp48 in the O–O bond-cleaving process.

4. Conclusions

The mechanism for O–O bond cleavage of dioxygen in MMO and RNR has been compared using the B3LYP method. The suggested mechanism for the O–O bond cleavage in RNR can be described as a path following first a non-radical tryptophan solution until an O–O distance of about 2.0 Å. At this point there is a crossing to another surface and an electron is transferred from Trp48 to the iron dimer, leading to a cationic Trp48 radical and a negatively charged iron dimer. This surface is then followed to the product **X**, which is an $Fe_2(III,IV)$ state. For MMO, where there is no second sphere tryptophan, the O–O bond cleavage is forced to follow the initial potential surface where the transition state is reached at a slightly higher energy than the crossing point between the two surfaces in RNR. This scenario is suggested to explain the experimentally found difference in rates between RNR and MMO, favoring RNR, supporting previous proposals [3]. The product **Q** for MMO is an $Fe_2(IV,IV)$ state. It should finally be stressed that the present calculations are not accurate enough to prove that the mechanism is as suggested but they support this possibility.

References

- [1] P. Nordlund, H. Eklund, *J. Mol. Biol.* 232 (1993) 123.
- [2] S.-K. Lee, J.D. Lipscomb, *Biochemistry* 38 (1999) 4423.
- [3] J. Baldwin, C. Krebs, B.A. Ley, D.E. Edmondson, B.H. Huynh, J.M. Bollinger Jr., *J. Am. Chem. Soc.* 122 (2000) 12195.
- [4] P.E.M. Siegbahn, M.R.A. Blomberg, *Chem. Rev.* 100 (2000) 421.
- [5] P.E.M. Siegbahn, M.R.A. Blomberg, *J. Phys. Chem. B* 105 (2001) 9375.
- [6] A.D. Becke, *Phys. Rev. A* 38 (1988) 3098; A.D. Becke, *J. Chem. Phys.* 98 (1993) 1372; A.D. Becke, *J. Chem. Phys.* 98 (1993) 5648.
- [7] P.J. Hay, W.R. Wadt, *J. Chem. Phys.* 82 (1985) 299.
- [8] JAGUAR 4.0, Schrödinger Inc., Portland, OR, 1991–2000.
- [9] M.R.A. Blomberg, P.E.M. Siegbahn, G.T. Babcock, *J. Am. Chem. Soc.* 120 (1998) 8812.
- [10] P.E.M. Siegbahn, *J. Inorg. Chem.* 38 (1999) 2880.
- [11] P.E.M. Siegbahn, *J. Comp. Chem.* 22 (2001) 1634.
- [12] P.E.M. Siegbahn, *Theor. Chem. Acc.* 105 (2001) 197.

- [13] J.M. Bollinger, C. Krebs, A. Vicol, S. Chen, B.A. Ley, D.E. Edmondson, B.H.J. Huynh, *J. Am. Chem. Soc.* 120 (1998) 1094.
- [14] U. Ryde, M.H.M. Olsson, K. Pierloot, B.O. Roos, *J. Mol. Biol.* 261 (1996) 586.
- [15] J.M. Bollinger, W.H. Tong, N. Ravi, B.H. Huynh, D.E. Edmondson, J. Stubbe, *J. Am. Chem. Soc.* 116 (1994) 8024;
J.M. Bollinger, W.H. Tong, N. Ravi, B.H. Huynh, D.E. Edmondson, J. Stubbe, *J. Am. Chem. Soc.* 116 (1994) 8015;
J.M. Bollinger, W.H. Tong, N. Ravi, B.H. Huynh, D.E. Edmondson, J. Stubbe, *J. Am. Chem. Soc.* 116 (1994) 8007.
- [16] B.E. Sturgeon, D. Burdi, S. Chen, B.-H. Huynh, D.E. Edmondson, J. Stubbe, B.M. Hoffman, *J. Am. Chem. Soc.* 118 (1996) 7551.
- [17] K.E. Liu, A.M. Valentine, D.L. Wang, B.H. Huynh, D.E. Edmondson, A. Salifoglou, S.J. Lippard, *J. Am. Chem. Soc.* 117 (1995) 10174.
- [18] K.E. Liu, D.L. Wang, B.H. Huynh, D.E. Edmondson, A. Salifoglou, S.J. Lippard, *J. Am. Chem. Soc.* 116 (1995) 7465.
- [19] A. Ehrenberg, P. Reichard, *J. Biol. Chem.* 247 (1972) 3485.
- [20] P. Nordlund, B.-M. Sjöberg, H. Eklund, *Nature* 345 (1990) 593.
- [21] M. Sivaraja, D.B. Goodwin, M. Smith, B.M. Hoffman, *Science* 245 (1989) 738.
- [22] M.R.A. Blomberg, P.E.M. Siegbahn, G.T. Babcock, M. Wikström, *J. Am. Chem. Soc.* 122 (2001) 12848.
- [23] C. Krebs, S. Chen, J. Baldwin, B.A. Ley, U. Patel, D.E. Edmondson, B.H. Huynh, J.M. Bollinger Jr., *J. Am. Chem. Soc.* 122 (2000) 12207.